Wiebke HEINS*, Pablo BALLESTEROS*, Christian BOHN*

GAIN-SCHEDULED STATE-FEEDBACK CONTROL FOR ACTIVE CANCELLATION OF MULTISINE DISTURBANCES WITH TIME-VARYING FREQUENCIES

SUMMARY

The paper presents a discrete-time LTV controller for the rejection of harmonic disturbances with time-verying based on a state-augmented observer-based state-feedback controller with a time-verying internal model and a scheduled state-feed back gain. The control design method is based on quadratic stability for LPV systems. The design is carried out in discrete time and the controller can easily be implemented on real-time hardware.

***Keywords**: active noise control, disturbance rejection, gain scheduling, linear parameter-varying systems, observers, state feedback*

DYSKRETNY REGULATOR LTV DO ELIMINACJI SKŁADOWYCH HARMONICZNYCH ZAKŁÓCEŃ ZE ZMIENNĄ W CZASIE CZĘSTOTLIWOŚCIĄ

W pracy przedstawiono dyskretny regulator LTV do eliminacji składowych harmonicznych zakłóceń. Wprowadzony regulator bazuje na sprzężeniu od zmiennych stanu z zależnym od czasu wewnętrznym modelem. Konstrukcja regulatora wykorzystuje własności stabilności układów LPV. Regulator został opisany równaniami dyskretnymi i może być łatwo zaimplementowany w układach czasu rzeczywistego.

***Słowa kluczowe**: aktywne sterowanie hałasem, redukcja zkłóceń, układ liniowy niestacjonarny, obserwator, sprzężenie od stanu*

1. INTRODUCTION AND MOTIVATION

The design of controllers for the rejection of multisine disturbances with time-varying frequencies is considered. The frequencies are assumed to be known. Such a control problem frequently arises in active noise and vibration control (ANC/AVC) in applications where the disturbances are caused by imbalances due to rotating or oscillating masses or periodically fluctuating excitations, e.g. the torque of a combustion engine, and the rotational speed is measured. Application examples are automobiles and aircrafts.

For the rejection of disturbances with time-varying frequencies, time-varying controllers that are automatically adjusted to the disturbance frequencies are usually used. Although time-invariant controllers might be sufficient in some applications [1], time-varying controllers usually result in a much better performance, particularly if the disturbance frequencies vary over fairly wide ranges. Such time-varying controllers can be constructed in several ways (see Sec. 2.1). The controller considered here consists of a state-augmented observer with a time-varying internal disturbance model and a scheduled state-feedback gain (see Sec. 3), as proposed in [2]. However, the controller of [2] was designed in continuous-time and only tested in simulation studies (on a very simple two-mass system) for a single-frequency disturbance. In this paper, the control design method is formulated in discrete-time and the controller is validated on an ANC headset for a disturbance signal consisting of four harmonics.

The remainder of this paper is organized as follows. In Sec. 2, an attempt is made to classify existing approaches and some general control design considerations are discussed. The state-augmented observer-based state-feedback approach is described in Sec. 3. In Sec. 4, the calculation of stabilizing state-feedback gains for time-varying systems in polytopic linear parameter-varying (pLPV) form is discussed. The application of this method for the rejection of harmonic disturbances is treated in Sec. 5. Real-time results are presented in Sec. 6. A discussion and some conclusions are given in Sec. 7.

2. CONTROLLER DESIGN: OVERVIEW, STABILITY AND IMPLEMENTATION ASPECTS

In this section, an overview of control approaches for the rejection of harmonic disturbances with time-varying frequencies is given (Sec. 2.1) and stability and implementation aspects are discussed (Secs. 2.2 and 2.3, respectively).

2.1. Overview and classification of control approaches

A common approach in ANC/AVC is adaptive filtering, where the filter weights are usually updated with the FxLMS algorithm [3]. In most cases, disturbance feedforward is used, although it is possible to use an adaptive filter in feedback control with a technique called "secondary path neutralization" [3], which is equivalent to internal model control [4].

* Institute of Electrical Information Technology, Clausthal University of Technology, Leibnizstr. 28, 38678 Clausthal-Zellerfeld, Germany

Another approach is to use gain scheduling, where the scheduling parameters are calculated from the disturbance frequencies. This can be further subdivided into indirect and direct scheduling methods. In indirect scheduling, the controller or part of it, e.g. a state-feedback or observer gain, is determined from a set of pre-computed quantities through interpolation or switching. For example, for LPV systems where the uncertain parameters are contained in a polytope, one controller is calculated for each vertex and the resulting controller is obtained from interpolation [5]. For the rejection of harmonic disturbances, a continuous-time LPV approach has been suggested in [6, 7] and tested in simulations for a single sinusoidal disturbance in [7]. Approaches based on observer-based state-feedback controllers are presented in [2, 8–15]. In [8–10], the observer gain is selected from a set of pre-computed gains by switching and in [11], the observer gain is calculated by interpolation. In [2, 12, 13] and this paper, the state-feedback gain is scheduled. In [14, 15], both the state feedback gain and the observer gain are scheduled.

In direct scheduling, the dependence of the controller on the scheduling parameter does not correspond to a simple interpolation or switching law. For example, for LPV systems where the parameter dependence is expressed as a linear fractional transformation (LFT), the uncertain parameters also enter the controller through an LFT [16]. For harmonic disturbances, LPV-LFT approaches have been suggested and applied in real time in [17–21]. Another example for direct scheduling is a controller based on a time-varying state estimator, e.g. a Kalman filter, where the scheduling parameters enter the controller through the recursive equations for the state estimate and the error covariance matrix. Such a controller is presented and compared to an indirect (interpolation) approach in [11].

2.2. Stability considerations

The design approaches can be classified as approaches that take stability into consideration and such that do not. The direct scheduling methods [11, 17–21] usually guarantee stability even for arbitrarily fast changes of the scheduling parameters. This also holds for the indirect scheduling LPV methods considered in [2, 6, 7, 13–15] and this paper. In indirect scheduling, however, the controllers or gains are sometimes pre-computed for fixed operating points and then interpolated in an ad-hoc fashion [8–10, 12]. Stability is then not guaranteed, although it might be expected that the system is stable for slow variations of the scheduling parameter. For the adaptive filtering approaches, only approximate stability results seem available to date [3, 22].

2.3. Implementation aspects

As mentioned above, the rejection of harmonic disturbances with time-varying frequencies is usually achieved through time-varying controllers. For the real-time implementation, such a time-varying controller has to be implemented in discrete time. An analogue implementation of a control algorithm would offer certain advantages (for example, anti-aliasing and reduction filters that increase the phase shift and therefore limit the achievable bandwidth, can be avoided). However, it is difficult to accurately realize arbitrary high-order time-invariant controllers using analogue electronics and even more difficult to incorporate adaptation or gain-scheduling mechanisms in an analogue implementation.

Sometimes, a control algorithm is designed in continuous-time and approximately discretized for the implementation. For a time-varying controller, this discretization would have to be carried out at each sampling instant. Particularly in LPV gain scheduling control, an approximate discretization is proposed [23]. However, this leads to a distortion of the frequency scale that shifts the controller poles to other frequencies. For the rejection of harmonic disturbances, it is required that the frequencies of the controller poles match the disturbance frequencies exactly. Therefore, a frequency distortion cannot be tolerated for controllers that are designed to suppress harmonic disturbances. Discretization methods that maintain the frequencies of the poles such as the zero-order-hold discretization or the matched pole-zero method [24] are computationally too expensive (calculation of a matrix exponential, calculations of poles at each sampling instant).

Also, in active noise and vibration control, the plant model is often obtained through system identification, which usually gives a discrete-time plant model. This alone motivates carrying out the whole design in discrete time (rather than converting the identified model into continuous-time, using a continuous-time design method and approximately discretizing the resulting controller).

In this context, it is not surprising that results of the continuous-time design methods [2, 6, 7, 11, 13–15] are usually only tested in simulations, whereas the design methods that are tested in real time [8–10, 12, 19–21] are formulated in discrete time. Exceptions are [17] and [18], where the design is carried out in continuous time and the controller is experimentally implemented. In [17], a very high sampling frequency of 40 kHz is chosen to reject a harmonic disturbance with a frequency up to 48 Hz (in fact, the authors of [17] state that they chose „the smallest [sampling time] available by the hardware"). In [18], the sampling time is not given, but the spectra are shown up to 1 kHz without any roll-off, also suggesting a very high sampling frequency. As mentioned above, it seems more natural to directly carry out the design in discrete time to avoid discretization issues. The design method presented in this paper is formulated in discrete time.

3. STATE-AUGMENTED OBSERVER-BASED STATE-FEEDBACK CONTROL

A standard linear state-feedback control law for the discrete-time LTI plant

$$\left[\begin{array}{c} \boldsymbol{x}_{\mathrm{p},k+1} \\ \hline \boldsymbol{y}_k \end{array}\right] = \left[\begin{array}{c|c} \boldsymbol{A}_\mathrm{p} & \boldsymbol{B}_\mathrm{p} \\ \hline \boldsymbol{C}_\mathrm{p} & 0 \end{array}\right] \left[\begin{array}{c} \boldsymbol{x}_{\mathrm{p},k} \\ \hline \boldsymbol{u}_k \end{array}\right] \tag{1}$$

with control input $\boldsymbol{u}$, output $\boldsymbol{y}$ and state vector $\boldsymbol{x}_{\mathrm{p}}$ is given by

$$\boldsymbol{u}_k = -\boldsymbol{K}_{\mathrm{p}} \boldsymbol{x}_{\mathrm{p},k} \tag{2}$$

where $\boldsymbol{K}_{\mathrm{p}}$ is the state-feedback gain. For improved disturbance rejection, it is often desired to include additional dynamics in the controller. This can be achieved by augmenting the plant with an output filter described by

$$\boldsymbol{x}_{\mathrm{M},k+1} = \left[\boldsymbol{A}_{\mathrm{M}} \mid \boldsymbol{B}_{\mathrm{M}}\right] \left[\begin{array}{c} \boldsymbol{x}_{\mathrm{M},k} \\ \hline \boldsymbol{y}_k \end{array}\right] \tag{3}$$

The additional dynamics can be chosen such that they describe the disturbances that the controller should reject, which corresponds to the well-known internal model principle [25]. The additional dynamics are therefore referred to as the "internal (disturbance) model". If, as in the control problem considered in this paper, the disturbance characteristics change over time, a time-varying internal model

$$\boldsymbol{x}_{\mathrm{M},k+1} = \left[\boldsymbol{A}_{\mathrm{M},k} \mid \boldsymbol{B}_{\mathrm{M}}\right] \left[\begin{array}{c} \boldsymbol{x}_{\mathrm{M},k} \\ \hline \boldsymbol{y}_k \end{array}\right] \tag{4}$$

can be used. Combining (1) and (4) leads to the overall, possibly time-varying, model

$$\left[\begin{array}{c} \boldsymbol{x}_{k+1} \\ \hline \boldsymbol{y}_k \end{array}\right] = \left[\begin{array}{c} \boldsymbol{x}_{\mathrm{M},k+1} \\ \boldsymbol{x}_{\mathrm{p},k+1} \\ \hline \boldsymbol{y}_k \end{array}\right] = \left[\begin{array}{cc|c} \boldsymbol{A}_{\mathrm{M},k} & \boldsymbol{B}_{\mathrm{M}}\boldsymbol{C}_{\mathrm{p}} & \boldsymbol{0} \\ \boldsymbol{0} & \boldsymbol{A}_{\mathrm{p}} & \boldsymbol{B}_{\mathrm{p}} \\ \hline \boldsymbol{0} & \boldsymbol{C}_{\mathrm{p}} & \boldsymbol{0} \end{array}\right] \left[\begin{array}{c} \boldsymbol{x}_{\mathrm{M},k} \\ \boldsymbol{x}_{\mathrm{p},k} \\ \hline \boldsymbol{u}_k \end{array}\right] = \tag{5}$$
$$= \left[\begin{array}{c|c} \boldsymbol{A}_k & \boldsymbol{B} \\ \hline \boldsymbol{C} & \boldsymbol{0} \end{array}\right] \left[\begin{array}{c} \boldsymbol{x}_k \\ \hline \boldsymbol{u}_k \end{array}\right]$$

The state-feedback control law then becomes

$$\boldsymbol{u}_k = -\boldsymbol{K}_k \boldsymbol{x}_k = -\left[\boldsymbol{K}_{\mathrm{M},k} \quad \boldsymbol{K}_{\mathrm{p},k}\right] \left[\begin{array}{c} \boldsymbol{x}_{\mathrm{M},k} \\ \boldsymbol{x}_{\mathrm{p},k} \end{array}\right] \tag{6}$$

where a time-varying feedback gain might be required to stabilize the time-varying system (5). The resulting time-varying controller is given by

$$\left[\begin{array}{c} \boldsymbol{x}_{\mathrm{M},k+1} \\ \hline \boldsymbol{u}_k \end{array}\right] = \left[\begin{array}{c|cc} \boldsymbol{A}_{\mathrm{M},k} & \boldsymbol{0} & \boldsymbol{B}_{\mathrm{M}} \\ \hline -\boldsymbol{K}_{\mathrm{M},k} & -\boldsymbol{K}_{\mathrm{p},k} & \boldsymbol{0} \end{array}\right] \left[\begin{array}{c} \boldsymbol{x}_{\mathrm{M},k} \\ \boldsymbol{x}_{\mathrm{p},k} \\ \boldsymbol{y}_k \end{array}\right] \tag{7}$$

The system matrix of the internal model, $\boldsymbol{A}_{\mathrm{M},k}$, is also the system matrix of the controller. Thus, $\boldsymbol{A}_{\mathrm{M}}$ can be used to prescribe controller poles. It can easily be verified that controller poles show up as zeros in the closed loop disturbance transfer functions. Therefore, controller poles can be chosen to correspond to disturbances that are to be suppressed. As mentioned above, this is the internal model principle [25]. This is utilized below (Sec. 5.1) for the rejection of harmonic disturbances. This argumentation, of course, only holds in the time-invariant case for which transfer functions and poles are defined (and only for controller poles that are not cancelled by plant zeros).

If the plant states are not available for feedback, they can be estimated with an observer given as

$$\hat{\boldsymbol{x}}_{\mathrm{p},k+1} = \left[\boldsymbol{A}_{\mathrm{p}} - \boldsymbol{L}\boldsymbol{C}_{\mathrm{p}} \mid \boldsymbol{L} \;\; \boldsymbol{B}_{\mathrm{p}}\right] \left[\begin{array}{c} \hat{\boldsymbol{x}}_{\mathrm{p},k} \\ \hline \boldsymbol{y}_k \\ \boldsymbol{u}_k \end{array}\right] = \tag{8}$$
$$= \left[\boldsymbol{A}_{\mathrm{obs}} \mid \boldsymbol{L} \;\; \boldsymbol{B}_{\mathrm{p}}\right] \left[\begin{array}{c} \hat{\boldsymbol{x}}_{\mathrm{p},k} \\ \hline \boldsymbol{y}_k \\ \boldsymbol{u}_k \end{array}\right]$$

where $\boldsymbol{L}$ is the observer gain and $\boldsymbol{A}_{\mathrm{obs}} = (\boldsymbol{A}_{\mathrm{p}} - \boldsymbol{L}\boldsymbol{C}_{\mathrm{p}})$ is the system matrix of the observer. Using the estimated states $\hat{\boldsymbol{x}}_{\mathrm{p}}$ instead of the true states $\boldsymbol{x}_{\mathrm{p}}$ results in the overall time-varying state-augmented observer-based controller

$$\left[\begin{array}{c} \boldsymbol{x}_{\mathrm{M},k+1} \\ \hat{\boldsymbol{x}}_{\mathrm{p},k+1} \\ \hline \boldsymbol{u}_k \end{array}\right] = \tag{9}$$
$$= \left[\begin{array}{cc|c} \boldsymbol{A}_{\mathrm{M},k} & \boldsymbol{0} & -\boldsymbol{B}_{\mathrm{M}} \\ -\boldsymbol{B}_{\mathrm{p}}\boldsymbol{K}_{\mathrm{M},k} & \boldsymbol{A}_{\mathrm{p}} - \boldsymbol{B}_{\mathrm{p}}\boldsymbol{K}_{\mathrm{p}} - \boldsymbol{L}\boldsymbol{C}_{\mathrm{p}} & -\boldsymbol{L} \\ \hline -\boldsymbol{K}_{\mathrm{M},k} & -\boldsymbol{K}_{\mathrm{p},k} & \boldsymbol{0} \end{array}\right] \left[\begin{array}{c} \boldsymbol{x}_{\mathrm{M},k} \\ \hat{\boldsymbol{x}}_{\mathrm{p},k} \\ \hline -\boldsymbol{y}_k \end{array}\right]$$

where a sign reversal in $\boldsymbol{B}_{\mathrm{M}}$, $\boldsymbol{L}$ and $\boldsymbol{y}_k$ has been introduced to write the controller in the standard negative feedback form. This controller structure is shown in Figure 1.

Introducing the observer error $\tilde{\boldsymbol{x}} = \boldsymbol{x}_{\mathrm{p}} - \hat{\boldsymbol{x}}_{\mathrm{p}}$, the dynamics of the closed loop system can be written as

$$\left[\begin{array}{c} \boldsymbol{x}_{k+1} \\ \hline \tilde{\boldsymbol{x}}_{k+1} \end{array}\right] = \left[\begin{array}{c} \boldsymbol{x}_{\mathrm{M},k+1} \\ \boldsymbol{x}_{\mathrm{p},k+1} \\ \hline \tilde{\boldsymbol{x}}_{k+1} \end{array}\right] =$$
$$= \left[\begin{array}{cc|c} \boldsymbol{A}_{\mathrm{M},k} & \boldsymbol{B}_{\mathrm{M}}\boldsymbol{C}_{\mathrm{p}} & \boldsymbol{0} \\ -\boldsymbol{B}_{\mathrm{p}}\boldsymbol{K}_{\mathrm{M},k} & \boldsymbol{A}_{\mathrm{p}} - \boldsymbol{B}_{\mathrm{p}}\boldsymbol{K}_{\mathrm{p},k} & \boldsymbol{B}_{\mathrm{p}}\boldsymbol{K}_{\mathrm{p},k} \\ \hline \boldsymbol{0} & \boldsymbol{0} & \boldsymbol{A}_{\mathrm{obs}} \end{array}\right] \left[\begin{array}{c} \boldsymbol{x}_{\mathrm{M},k} \\ \boldsymbol{x}_{\mathrm{p},k} \\ \hline \tilde{\boldsymbol{x}}_k \end{array}\right] = \tag{10}$$
$$= \left[\begin{array}{c|c} \boldsymbol{A}_{\mathrm{sfb},k} & \boldsymbol{B}\boldsymbol{K}_k \\ \hline \boldsymbol{0} & \boldsymbol{A}_{\mathrm{obs}} \end{array}\right] \left[\begin{array}{c} \boldsymbol{x}_k \\ \hline \tilde{\boldsymbol{x}}_k \end{array}\right]$$

and thus can be separated into the time-varying dynamics $\boldsymbol{A}_{\mathrm{sfb},k} = (\boldsymbol{A}_k - \boldsymbol{B}\boldsymbol{K}_k)$ of the plant under state feedback and the time-invariant dynamics $\boldsymbol{A}_{\mathrm{obs}}$ of the observer error. Choosing a constant observer gain such that $\boldsymbol{A}_{\mathrm{obs}}$ is stable and a time-varying state-feedback gain such that the time-varying dynamics described by $\boldsymbol{A}_{\mathrm{sfb},k}$ are stable therefore guarantees overall stability of the closed loop system. In the following section it is described how a time-varying stabilizing feedback gain can be found for systems where the matrix $\boldsymbol{A}_k$ is in pLPV form.

4. GAIN-SCHEDULED STATE-FEEDBACK CONTROL FOR PLPV MODELS

The controller structure described in Sec. 3 requires a time-varying state-feedback gain $\boldsymbol{K}_k$ that has to be computed on-line in every sampling instant or, more specifically, whenever $\boldsymbol{A}_k$ changes. If the models of plant and disturbance are given in the form of a pLPV system, this can be reduced to interpolation between fixed state-feedback gains which can be pre-computed off-line. The theoretical background for this approach is described in this section.

4.1. State feedback design for pLPV systems based on quadratic stability

A pLPV system is of the form

$$\boldsymbol{x}_{k+1} = \boldsymbol{A}(\boldsymbol{\theta})\boldsymbol{x}_k \tag{11}$$

where the system matrix depends affinely on a parameter vector $\boldsymbol{\theta}$,

$$\boldsymbol{A}(\boldsymbol{\theta}) = \boldsymbol{A}_0 + \theta_1 \boldsymbol{A}_1 + \ldots + \theta_N \boldsymbol{A}_N \tag{12}$$

with constant matrices $\boldsymbol{A}_i$. The parameter vector $\boldsymbol{\theta}$ varies in a polytope Θ with M vertices $\boldsymbol{v}_j \in \mathbf{R}^N$. A point $\boldsymbol{\theta} \in \Theta$ can be written as a convex combination of vertices, i.e. there exists a coordinate vector $\boldsymbol{\lambda} = [\lambda_1 \ldots \lambda_M]^{\mathrm{T}} \in \mathbf{R}^M$ such that $\boldsymbol{\theta}$ can be written as

$$\boldsymbol{\theta} = \sum_{j=1}^{M} \lambda_j \boldsymbol{v}_j \quad \text{with} \quad \lambda_j \geq 0, \quad \sum_{j=1}^{M} \lambda_j = 1 \tag{13}$$

Defining $\boldsymbol{A}_{\mathrm{v},j} = \boldsymbol{A}(\boldsymbol{v}_j)$ for $j = 1, ..., M$, $\boldsymbol{A}(\boldsymbol{\theta})$ can be represented as

$$\boldsymbol{A}(\boldsymbol{\theta}) = \boldsymbol{A}(\boldsymbol{\lambda}) = \lambda_1 \boldsymbol{A}_{\mathrm{v},1} + \lambda_2 \boldsymbol{A}_{\mathrm{v},2} + \ldots + \lambda_M \boldsymbol{A}_{\mathrm{v},M} \tag{14}$$

The matrices $\boldsymbol{A}_{\mathrm{v},j}$ can be considered as system matrices of LTI *vertex systems*

$$\boldsymbol{x}_{k+1} = \boldsymbol{A}_{\mathrm{v},j} \boldsymbol{x}_k, \quad j = 1, \ldots, M \tag{15}$$

and the current system (11) is a convex combination of the vertex systems in (15).

A pLPV system as in (11) is called quadratically stable [26] if and only if there exists a symmetric positive definite matrix $\boldsymbol{P}$ such that

$$\boldsymbol{A}^{\mathrm{T}}(\boldsymbol{\theta})\boldsymbol{P}\boldsymbol{A}(\boldsymbol{\theta}) - \boldsymbol{P} < 0 \quad \text{for all} \quad \boldsymbol{\theta} \in \Theta \tag{16}$$

or equivalently (via the Schur complement [27])

$$\begin{bmatrix} \boldsymbol{P} & \boldsymbol{P}\boldsymbol{A}(\boldsymbol{\theta}) \\ \boldsymbol{A}(\boldsymbol{\theta})^{\mathrm{T}}\boldsymbol{P} & \boldsymbol{P} \end{bmatrix} > 0 \quad \text{for all} \quad \boldsymbol{\theta} \in \Theta \tag{17}$$

where "> 0" and "< 0" indicate positive and negative definiteness, respectively. Since (16) and (17) have to hold for every $\boldsymbol{\theta} \in \Theta$, this constitutes an infinite set of linear matrix inequalities (LMIs), which is computationally intractable. By the following result, it is possible to use a finite set of inequalities. It holds that a pLPV system in the form of (11) is quadratically stable for every $\boldsymbol{\theta} \in \Theta$ if and only if there exists a symmetric positive definite matrix $\boldsymbol{P}$ such that (16), or equivalently (17), holds for all vertices $\boldsymbol{v}_j$ of Θ, that is

$$\boldsymbol{A}_{\mathrm{v},j}^{\mathrm{T}} \boldsymbol{P} \boldsymbol{A}_{\mathrm{v},j} - \boldsymbol{P} < 0, \quad j = 1, \ldots, M \tag{18}$$

or, equivalently,

$$\begin{bmatrix} \boldsymbol{P} & \boldsymbol{P}\boldsymbol{A}_{\mathrm{v},j} \\ \boldsymbol{A}_{\mathrm{v},j}^{\mathrm{T}}\boldsymbol{P} & \boldsymbol{P} \end{bmatrix} > 0, \quad j = 1, \ldots, M \tag{19}$$

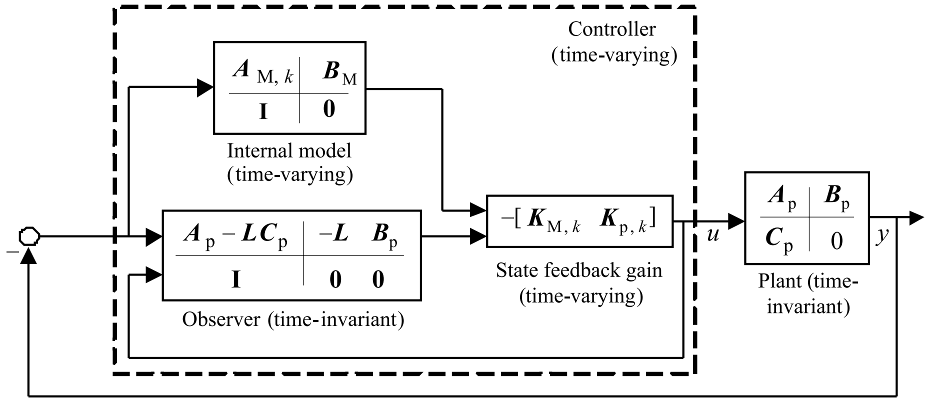

Fig. 1. Time-varying state-augmented observer-based state-feedback controller

This result is based on one single quadratic Lyapunov function that assures stability for the whole parameter space Θ. Therefore, $\boldsymbol{\theta}$ is allowed to change arbitrarily fast with time and $\boldsymbol{\theta}$ and $\boldsymbol{\lambda}$ can explicitly be assumed time-varying and denoted as $\boldsymbol{\theta}_k$ and $\boldsymbol{\lambda}_k$, respectively. A proof is given in [26].

These results can be applied to the design of parameter-dependent state-feedback gains. A system of the form

$$\boldsymbol{x}_{k+1} = \boldsymbol{A}(\theta_k)\boldsymbol{x}_k + \boldsymbol{B}\boldsymbol{u}_k \tag{20}$$

is considered and the objective is to find a state-feedback gain $\boldsymbol{K}(\boldsymbol{\theta}_k)$ that quadratically stabilizes the closed loop system

$$\boldsymbol{x}_{k+1} = \left(\boldsymbol{A}(\theta_k) - \boldsymbol{B}\boldsymbol{K}(\theta_k)\right)\boldsymbol{x}_k \tag{21}$$

From the above result it follows that it suffices to find a single symmetric positive definite matrix $\boldsymbol{P}$ and a finite set of matrices $\boldsymbol{K}_{\mathrm{v},j}$ such that

$$\begin{bmatrix} \boldsymbol{P} & \boldsymbol{P}\left(\boldsymbol{A}_{\mathrm{v},j} - \boldsymbol{B}\boldsymbol{K}_{\mathrm{v},j}\right) \\ \left(\boldsymbol{A}_{\mathrm{v},j} - \boldsymbol{B}\boldsymbol{K}_{\mathrm{v},j}\right)^{\mathrm{T}}\boldsymbol{P} & \boldsymbol{P} \end{bmatrix} > 0, \quad j = 1, ..., M \tag{22}$$

Then, $\boldsymbol{K}(\theta_k)$ has to be chosen as

$$\boldsymbol{K}(\theta_k) = \sum_{j=1}^{M} \lambda_{j,k}\boldsymbol{K}_{\mathrm{v},j} = \boldsymbol{K}(\lambda_k) \tag{23}$$

because then it holds that

$$\begin{aligned} \boldsymbol{A}(\theta_k) - \boldsymbol{B}\boldsymbol{K}(\theta_k) &= \sum_{j=1}^{M} \lambda_{j,k}\boldsymbol{A}_{\mathrm{v},j} - \boldsymbol{B}\sum_{j=1}^{M} \lambda_{j,k}\boldsymbol{K}_{\mathrm{v},j} = \\ &= \sum_{j=1}^{M} \lambda_{j,k}\left(\boldsymbol{A}_{\mathrm{v},j} - \boldsymbol{B}\boldsymbol{K}_{\mathrm{v},j}\right) \end{aligned} \tag{24}$$

and therefore quadratic stability of (21) is implied due to the results presented above.

4.2. Computation of state-feedback gains for the vertex systems

In this section, sufficient conditions that guarantee closed loop stability and a certain H_2 performance level for the controlled vertex systems that can be used to calculate state-feedback gains for the vertex systems are derived. To use an H_2 performance level, an additional performance input is introduced that enters the state update for each vertex system of the pLPV-system in (20). This input can be interpreted as process noise. For every j = 1, ..., M, this yields

$$\boldsymbol{x}_{k+1} = \boldsymbol{A}_{\mathrm{v},j}\boldsymbol{x}_k + \boldsymbol{B}\boldsymbol{u}_k + \boldsymbol{w}_k \tag{25}$$

As a performance output, the artificial signal

$$z_k = \begin{bmatrix} \boldsymbol{Q}^{1/2}\boldsymbol{x}_k \\ \boldsymbol{R}^{1/2}\boldsymbol{u}_k \end{bmatrix} \tag{26}$$

is defined that weights the states and the control signal with matrices $\boldsymbol{Q}^{1/2}$ and $\boldsymbol{R}^{1/2}$ respectively. The objective then is to find state-feedback gains $\boldsymbol{K}_{\mathrm{v},j}$ that stabilize the system and minimize the H_2 norm of the transfer path from $\boldsymbol{w}_k$ to $\boldsymbol{z}_k$, when the control signal $\boldsymbol{u}_k$ in (25) and (26) is chosen as

$$\boldsymbol{u}_k = -\boldsymbol{K}_{\mathrm{v},j}\boldsymbol{x}_k \tag{27}$$

This objective can be stated as the minimization of the H_2 norm of the system

$$z = \boldsymbol{G}\boldsymbol{w} \tag{28}$$

which has the state-space representation

$$\begin{aligned} &\begin{bmatrix} \boldsymbol{x}_{k+1} \\ z_k \end{bmatrix} = \left[\begin{array}{c|c} \tilde{\boldsymbol{A}} & \tilde{\boldsymbol{B}} \\ \hline \tilde{\boldsymbol{C}} & \boldsymbol{0} \end{array}\right]\begin{bmatrix} \boldsymbol{x}_k \\ \boldsymbol{w}_k \end{bmatrix}, \quad \tilde{\boldsymbol{A}} = \boldsymbol{A}_{\mathrm{v},j} - \boldsymbol{B}\boldsymbol{K}_{\mathrm{v},j}, \\ &\tilde{\boldsymbol{B}} = \mathbf{I}, \quad \tilde{\boldsymbol{C}} = \begin{bmatrix} \boldsymbol{Q}^{1/2} \\ -\boldsymbol{R}^{1/2}\boldsymbol{K}_{\mathrm{v},j} \end{bmatrix} \end{aligned} \tag{29}$$

If the system is stable, the H_2 norm of this discrete-time LTI system is given by

$$\|\boldsymbol{G}\|_2^2 = \operatorname{trace} \tilde{\boldsymbol{C}}\boldsymbol{W}_c\tilde{\boldsymbol{C}}^{\mathrm{T}} \tag{30}$$

where the controllability gramian $\boldsymbol{w}_c$ satisfies the discrete-time Lyapunov equation

$$\tilde{\boldsymbol{A}}\boldsymbol{W}_c\tilde{\boldsymbol{A}}^{\mathrm{T}} - \boldsymbol{W}_c + \tilde{\boldsymbol{B}}\tilde{\boldsymbol{B}}^{\mathrm{T}} = 0 \tag{31}$$

Therefore, if there exist symmetric positive definite matrices $\boldsymbol{P}$ and $\boldsymbol{W}$ such that

$$\tilde{\boldsymbol{A}}\boldsymbol{P}\tilde{\boldsymbol{A}}^{\mathrm{T}} - \boldsymbol{P} + \tilde{\boldsymbol{B}}\tilde{\boldsymbol{B}}^{\mathrm{T}} < 0 \tag{32}$$

$$\boldsymbol{W} - \tilde{\boldsymbol{C}}\boldsymbol{P}\tilde{\boldsymbol{C}}^{\mathrm{T}} > 0 \tag{33}$$

$$\operatorname{trace} \boldsymbol{W} < \gamma^2 \tag{34}$$

then it follows that $\|\boldsymbol{G}\|_2 < \gamma$ for $\gamma > 0$. Through the Schur complement, (32) and (33) can be transformed to

$$\begin{bmatrix} \boldsymbol{P} & \boldsymbol{P}\tilde{\boldsymbol{A}}^{\mathrm{T}} \\ \tilde{\boldsymbol{A}}\boldsymbol{P} & \boldsymbol{P} - \tilde{\boldsymbol{B}}\tilde{\boldsymbol{B}}^{\mathrm{T}} \end{bmatrix} > 0 \tag{35}$$

$$\begin{bmatrix} \boldsymbol{W} & \tilde{\boldsymbol{C}}\boldsymbol{P} \\ \boldsymbol{P}\tilde{\boldsymbol{C}}^{\mathrm{T}} & \boldsymbol{P} \end{bmatrix} > 0 \tag{36}$$

Introducing

$$\tilde{\boldsymbol{Q}} = \begin{bmatrix} \boldsymbol{Q}^{1/2} \\ \boldsymbol{0} \end{bmatrix}, \quad \tilde{\boldsymbol{R}} = \begin{bmatrix} \boldsymbol{0} \\ \boldsymbol{R}^{1/2} \end{bmatrix}, \quad \boldsymbol{Y}_{\mathrm{v},j} = \boldsymbol{K}_{\mathrm{v},j}\boldsymbol{P} \qquad (37)$$

it follows that if solutions for the matrix variables $\boldsymbol{P}$, $\boldsymbol{W}$ and $\boldsymbol{Y}_{\mathrm{v},j}$, $j = 1, ..., M$, can be found that satisfy the $2M+1$ LMIs

$$\begin{bmatrix} \boldsymbol{P} & \boldsymbol{P}\boldsymbol{A}_{\mathrm{v},j}^{\mathrm{T}} - \boldsymbol{Y}_{\mathrm{v},j}^{\mathrm{T}}\boldsymbol{B}^{\mathrm{T}} \\ \boldsymbol{A}_{\mathrm{v},j}\boldsymbol{P} - \boldsymbol{B}\boldsymbol{Y}_{\mathrm{v},j} & \boldsymbol{P} - \mathbf{I} \end{bmatrix} > 0, \quad j = 1, ..., M \qquad (38)$$

$$\begin{bmatrix} \boldsymbol{W} & \tilde{\boldsymbol{Q}}\boldsymbol{P} - \tilde{\boldsymbol{R}}\boldsymbol{Y}_{\mathrm{v},j} \\ \boldsymbol{P}\tilde{\boldsymbol{Q}}^{\mathrm{T}} - \boldsymbol{Y}_{\mathrm{v},j}^{\mathrm{T}}\tilde{\boldsymbol{R}}^{\mathrm{T}} & \boldsymbol{P} \end{bmatrix} > 0, \quad j = 1, ..., M \qquad (39)$$

$$\operatorname{trace} \boldsymbol{W} < \gamma^2 \qquad (40)$$

then the system $\boldsymbol{G}$ has an H_2 norm bounded by γ. From the solutions $\boldsymbol{P}$ and $\boldsymbol{Y}_{\mathrm{v},j}$, the state-feedback gain for each vertex system can be calculated as

$$\boldsymbol{K}_{\mathrm{v},j} = \boldsymbol{Y}_{\mathrm{v},j}\boldsymbol{P}^{-1} \qquad (41)$$

Quadratic stability is then implied for each closed loop vertex system because of (32). In order to guarantee quadratic stability for the whole parameter space, solutions for the matrix variables $\boldsymbol{P}$ and $\boldsymbol{W}$ in (38)–(40) have to be the *same* for all vertex systems. Therefore, if solutions are found, also the performance bound γ is guaranteed for every fixed $\boldsymbol{\theta}$ in the parameter space Θ, since it depends only on $\boldsymbol{P}$ and $\boldsymbol{W}$.

Once state-feedback gains are found for the vertex systems, in any instant of time of a realization of the pLPV-system (20) with $\boldsymbol{\theta}_k \in \Theta$, a state-feedback gain can be found via interpolation according to (23). Quadratic stability and the desired H_2 performance of the closed loop system (21) are guaranteed. The question of how to compute the coordinates $\lambda_k = \left[\lambda_{1,k} \ldots \lambda_{M,k}\right]^{\mathrm{T}} \in \mathbf{R}^M$ with the properties described in (13) depends on the specific polytope Θ. The case of an N-dimensional cuboid will be considered in detail in Sec. 5.3.

5. APPLICATION FOR THE REJECTION OF HARMONIC DISTURBANCES

In this section, the method described in Sec. 4 is applied to the case of a harmonic multisine disturbance. Specific system models and the transformation that leads to a pLPV system are presented. Also the computation of the coordinates required for interpolation is briefly reviewed.

5.1. Internal model for harmonic disturbances

As discussed in Sec. 3, the internal model can be used to determine controller poles (that show up as zeros in the disturbance transfer functions). For complete asymptotic rejection of harmonic disturbances with frequency f, a complex conjugate controller pole pair has to be placed at $\pm j2\pi fT$, where T is the sampling time. This can be achieved with the internal model

$$\boldsymbol{A}_{\mathrm{M}} = \begin{bmatrix} 0 & 1 \\ -1 & 2\cos(2\pi fT) \end{bmatrix}, \quad \boldsymbol{B}_{\mathrm{M}} = \begin{bmatrix} 0 \\ 1 \end{bmatrix} \qquad (42)$$

The disturbance considered here is assumed to be a multisine with N individual components. The frequency of the i-th component at each sampling instant k is denoted by $f_{i,k}$. The frequencies are assumed to vary in intervals $[f_{i,\min}, f_{i,\max}] \subseteq [0,\ 0.5f_s)$, where $f_s = 1/T$ denotes the sampling frequency. The overall internal model can then be obtained by combining individual internal models of the form (42) according to

$$\boldsymbol{A}_{\mathrm{M},k} = \begin{bmatrix} \boldsymbol{A}_{\mathrm{M}_1,k} & \cdots & \boldsymbol{0} \\ \vdots & \ddots & \vdots \\ \boldsymbol{0} & \cdots & \boldsymbol{A}_{\mathrm{M}_N,k} \end{bmatrix},$$
$$\boldsymbol{A}_{\mathrm{M}_i,k} = \begin{bmatrix} 0 & 1 \\ -1 & 2\theta_{i,k} \end{bmatrix}, \quad \theta_{i,k} = \cos(2\pi f_{i,k}T) \qquad (43)$$

$$\boldsymbol{B}_{\mathrm{M}} = \begin{bmatrix} \boldsymbol{B}_{\mathrm{M}_1} \\ \vdots \\ \boldsymbol{B}_{\mathrm{M}_N} \end{bmatrix}, \quad \boldsymbol{B}_{\mathrm{M}_i} = \begin{bmatrix} 0 \\ 1 \end{bmatrix}, \quad i = 1, ..., N \qquad (44)$$

In this internal model, controller poles are placed on the unit circle, which leads to a controller with infinite gain at the disturbance frequencies. In practice, it is sufficient and possibly numerically better to obtain a very high (not necessarily infinite) controller gain. The poles can therefore also be placed inside the unit disc and very close to the unit circle, i.e. at $(1 - \varepsilon)\exp(\pm j2\pi fT)$, where ε is a very small positive number.

The argumentation based on controller poles is technically only correct for the time-invariant case. If a time-varying internal model is used, it is not easy to interpret what happens when the internal model changes. Conceptually, the argument that the controller has high (infinite) gain at the disturbance frequencies that are to be rejected should still hold. It is confirmed by experiments (see Sec. 6) that even for fairly fast changes of the disturbance frequencies, excellent disturbance rejection is achieved. For very fast changes the disturbance attenuation performance gets worse, but stability is guaranteed even for arbitrarily fast changes of the internal model due to the design approach of Sec. 4.

Also, the variations of the disturbance frequency are not taken into account in the internal model used here.

A "correct" model (that takes the variations into account) would involve system matrices $A_{M_{i},k}$ of the form

$$A_{M_{i},k}=\begin{bmatrix}\cos(2\pi f_{i,k}T) & \sin(2\pi f_{i,k}T)\\ -\sin(2\pi f_{i,k}T) & \cos(2\pi f_{i,k}T)\end{bmatrix} \tag{45}$$

This aspect is also discussed in [2] for the continuous-time case, where a "correct" model is used, c.f. eqs. (2), (3), (11) and (12) in [2]. Nevertheless the "incorrect" model (42) is used here since it is easier to transform this model to pLPV form than the "correct" model (45) As will be shown in the next section, in order to avoid a nonlinear dependence on the parameter space, not the frequency itself, but its cosine is considered as the system parameter. For the simplified model (42) this leads to a dimension of the parameter space which corresponds to the number of frequencies. For the same approach, the exact model (45) still inherits a non-affine dependence because of the presence of the sine. Any approach to transform this increases the dimension of the parameter space (and therefore the computational complexity and conservatism of the controller design) significantly. This problem only arises in the discrete-time setting. In the continuous-time case, the "correct" model can easily be transformed to pLPV form [2].

The use of the simpler internal model might have an effect on the disturbance attenuation for fast changes of the frequencies. However, for fast changes of the disturbance frequency, it is expected that in a real application other effects are more dominant than the "incorrect" internal model: There will always be a delay between the measured frequency used in the controller and the true frequency. Also, if the disturbance and the control signal do not enter at exactly the same point and the disturbance frequency varies, it is unclear which frequency "is present" at the point where the control signal enters the plant at a certain time. As shown in Sec. 3, closed loop stability is not affected by the choice of the internal model.

5.2. Transformation to pLPV form

For the design procedure a representation of the system matrix A_k of the augmented system (5) in the form of a pLPV system is needed. The necessary transformations are described in this section.

The matrix $A_{M,k}$ from (43) is rewritten as

$$A_{M,k}=A_M(\theta_k)=A_{M_0}+\theta_{1,k}A_{M_i}+\ldots+\theta_{N,k}A_{M_N} \tag{46}$$

which corresponds to the representation of (12), where, with $\theta_{i,k}$ from (43),

$$A_{M_0}=\begin{bmatrix}A_{M_0,1} & \cdots & \mathbf{0}\\ \vdots & \ddots & \vdots\\ \mathbf{0} & \cdots & A_{M_0,N}\end{bmatrix},\quad A_{M_0,i}=\begin{bmatrix}0 & 1\\ -1 & 0\end{bmatrix} \tag{47}$$

The entries of the matrices A_{M_i} are all zero except for

$$A_{M_i}(2i,2i)=2,\quad i=1,\ldots,N \tag{48}$$

The system matrix A_k can then be written as

$$A_k=A(\theta_k)=A_0+\theta_{1,k}A_1+\ldots+\theta_{N,k}A_N \tag{49}$$

$$A_0=\begin{bmatrix}A_{M_0} & B_M C_p\\ \mathbf{0} & A_p\end{bmatrix},\quad A_i=\begin{bmatrix}A_{M_i} & \mathbf{0}\\ \mathbf{0} & \mathbf{0}\end{bmatrix} \tag{50}$$

Due to the sampling theorem, it holds that $0\le 2\pi f_{i,k}T<\pi$ for all i = 1, ..., N and therefore the parameters $\theta_{i,k}$ vary in a range of $[\theta_{i,\min}, \theta_{i,\max}]$ with

$$\theta_{i,\min}=\cos(2\pi f_{i,\max}T),\quad \theta_{i,\max}=\cos(2\pi f_{i,\min}T) \tag{51}$$

since the cosine is monotonically decreasing on $[0, \pi]$. Therefore, the parameter vector θ_k varies in an N-dimensional cuboid, the "parameter box"

$$\begin{aligned}\Theta=&[\theta_{1,\min},\theta_{1,\max}]\times[\theta_{2,\min},\theta_{2,\max}]\times\\ &\ldots\times[\theta_{N,\min},\theta_{N,\max}]\end{aligned} \tag{52}$$

with $M = 2^N$ vertices.

5.3. Controller implementation

Once the pLPV representation of the considered system is found, state-feedback gains for vertex systems can be computed following the method of Sec. 4.2. Since the plant is LTI, the observer required for the estimation of the plant states can be designed off-line with a standard method (e.g. LQR or pole placement). The controller is then implemented according to Sec. 3 and the scheme given in Figure 2. The system matrix $A_{M,k}$ is updated in every sampling instant directly with the measured frequencies, while the state-feedback gain K_k is obtained by the interpolation (23).

The coordinates λ_k required for interpolation can be computed following the scheme that is introduced in [5] and generalized and implemented for an arbitrary number of vertices in the LMI Control Toolbox for Matlab [28]. Another way of implementation is proposed here that is suitable for real-time implementation purposes where variables have to be pre-initialized with fixed dimensions. In [29], a compact way of writing the calculation scheme is presented, on which the scheme proposed here is based. If the order of vertices is not changed, every approach leads to the same coordinates.

The i-th entry $v_{j,i}$ of a vertex $v_j=[v_{j,1}\ \ldots\ v_{j,N}]^T$ of the parameter box Θ is either the lower bound $\theta_{i,\min}$ or the upper bound $\theta_{i,\max}$ of $\theta_{i,k}$. Now, $2N$ vectors

$$\begin{aligned}b_{i_{\max}}&=[b_{i_{\max},1}\cdots b_{i_{\max},N}]^T,\\ b_{i_{\min}}&=[b_{i_{\min},1}\cdots b_{i_{\min},M}]^T\end{aligned} \tag{53}$$

are pre-computed such that

$$b_{i_{\max},j} = \begin{cases} 1/(\theta_{i,\max} - \theta_{i,\min}), & \text{if} \quad v_{j.i} = \theta_{i,\max} \\ 0, & \text{if} \quad v_{j.i} = \theta_{i,\min} \end{cases} \tag{54}$$

$$b_{i_{\min},j} = \begin{cases} 1/(\theta_{i,\max} - \theta_{i,\min}), & \text{if} \quad v_{j.i} = \theta_{i,\min} \\ 0, & \text{if} \quad v_{j.i} = \theta_{i,\max} \end{cases} \tag{55}$$

The following steps are then carried out on-line in every sampling instant:

1. $\theta_{i,k} = \cos(2\pi f_{i,k} T), \quad i = 1, ..., N$ (56)

2. $c_{i_{\max},k} = \theta_{i,k} - \theta_{i,\min}, \quad c_{i_{\min},k} = \theta_{i,\max} - \theta_{i,k},$
$i = 1, ..., N$ (57)

3. $\lambda_{j,k} = \prod_{i=1}^{N} (b_{i_{\max},j} c_{i_{\max},k} + b_{i_{\min},j} c_{i_{\min},k}),$
$j = 1, ..., M$ (58)

The choice of the coordinates $\boldsymbol{\lambda}_k$ is not unique for a polytope with more than N+1 vertices. Another interpolation scheme might lead to different properties of the resulting controller.

The resulting controller is shown in Figure 2. It corresponds to the state-augmented observer-based state-feedback controller discussed in Sec. 3 (and shown in Fig. 1), augmented with the updating mechanism described in this section.

6. REAL-TIME RESULTS

The obtained controller is tested experimentally on an ANC headset (Sennheiser PXC 300). The experimental setup is shown in Figure 3. An external loudspeaker generates the harmonic disturbance. The headset has one microphone in each ear cup. The objective is to cancel the disturbance with the loudspeakers of the headset. An anti-aliasing filter is applied to the output signal and a reconstruction filter to the control input. The control algorithm is implemented on a rapid control prototyping unit (dSpace MicroAutoBox).

In this setup, the plant introduced in (1) corresponds to the transfer function from the output to the input of the control unit. It is experimentally determined by exciting the system with a multisine test signal, recording input and output. The transfer function can be estimated using a standard black-box technique (oe). All usual methods (arx, oe, n4sid) resulted in models that were suitable for control design, so the choice of the method was not crucial. If a transfer function model is identified, it has to be converted to a state-space representation.

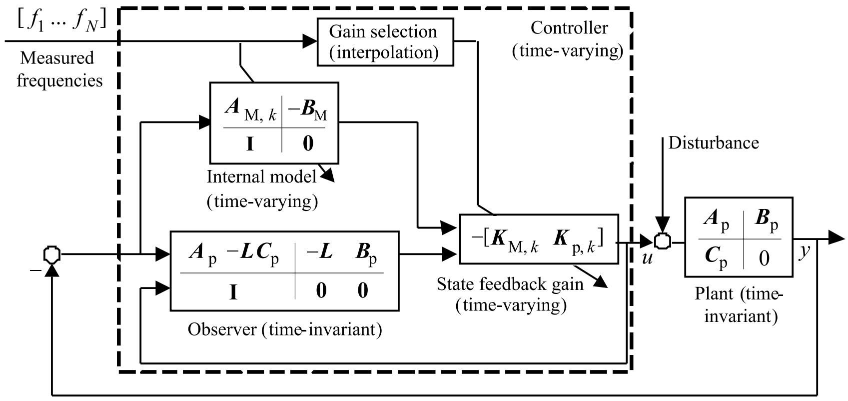

Fig. 2. Feedback control structure

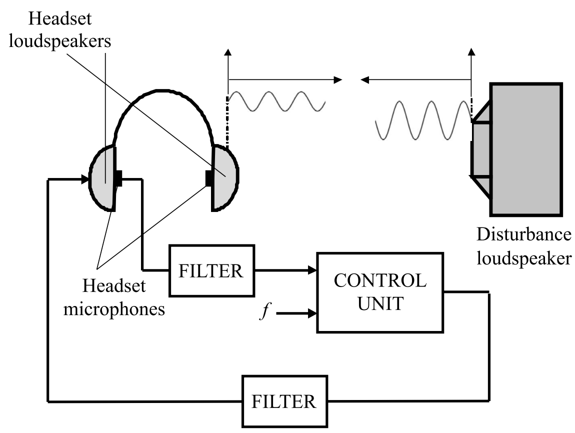

Fig. 3. ANC System

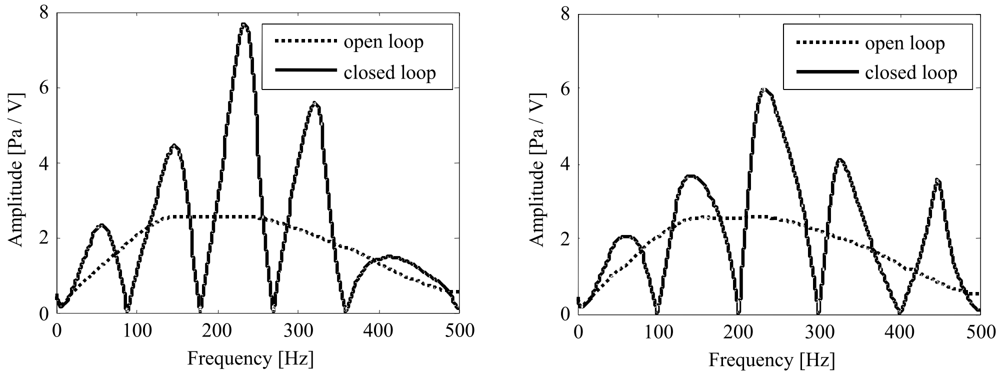

Fig. 4. Open loop and closed loop amplitude frequency responses for disturbance frequencies of 90 Hz, 180 Hz, 270 Hz and 360 Hz (left) and 100 Hz, 200 Hz, 300 Hz and 400 Hz (right)

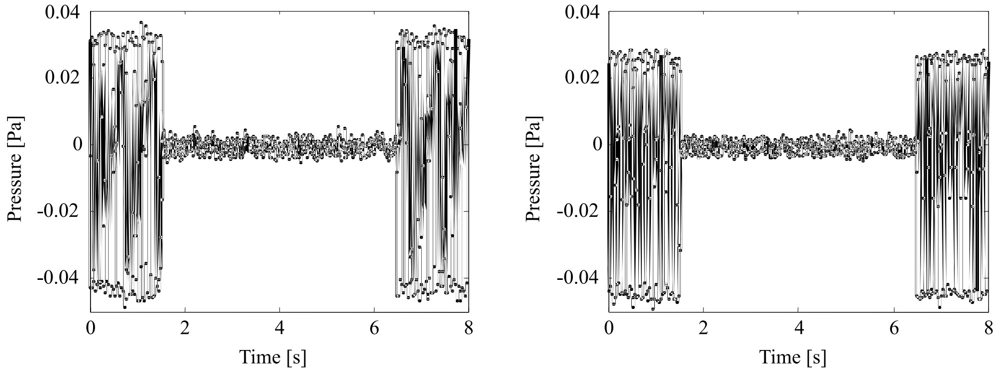

Fig. 5. Microphone signal for fixed frequencies of 90 Hz, 180 Hz, 270 Hz, 360 Hz (left) and 100 Hz, 200 Hz, 300 Hz and 400 Hz (right). The control sequence is off/on/off

The identified system is of 12th order. The disturbance applied is a sum of four harmonically related sine signals with fundamental frequency between 90 Hz and 100 Hz. This gives an internal model of 8th order and a parameter box in $\mathbf{R}^4$ with 16 vertices. The resulting controller is of 20th order. A sampling frequency of 1 kHz was chosen such that the Nyquist frequency of 500 Hz is still higher than the highest disturbance frequency of 400 Hz (in the fourth harmonic). The control algorithm has been implemented for both sides, but only results for the right side are shown.

Figure 4 shows the amplitude frequency response in open loop and closed loop. At the specified disturbance frequencies, the amplitude response is zero, which corresponds to complete asymptotic disturbance cancellation. This is confirmed by Figure 5, which shows the corresponding real-time results. Figure 4 also shows that disturbance amplification occurs in the frequency ranges between the rejected frequencies. This effect is due to Bode's sensitivity integral ("waterbed" effect) [30]. It might cause problems in applications where significant background noise is present.

In Figure 6, results for a time-varying fundamental frequency are shown. The fundamental frequency decreases linearly from 100 Hz to 90 Hz and then increases back to 100 Hz. This is repeated four times, every time in a shorter

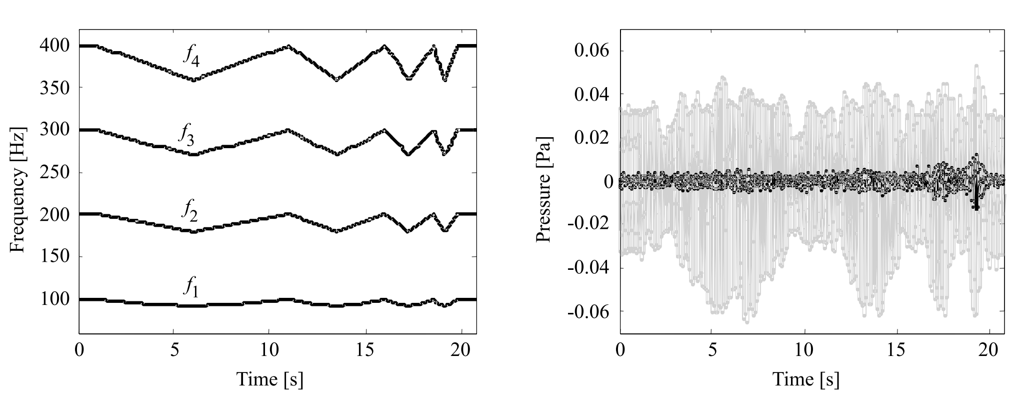

Fig. 6. Results for time-varying disturbance frequencies: Frequency variations (left) and microphone signal (right) in open loop (gray) and closed loop (black)

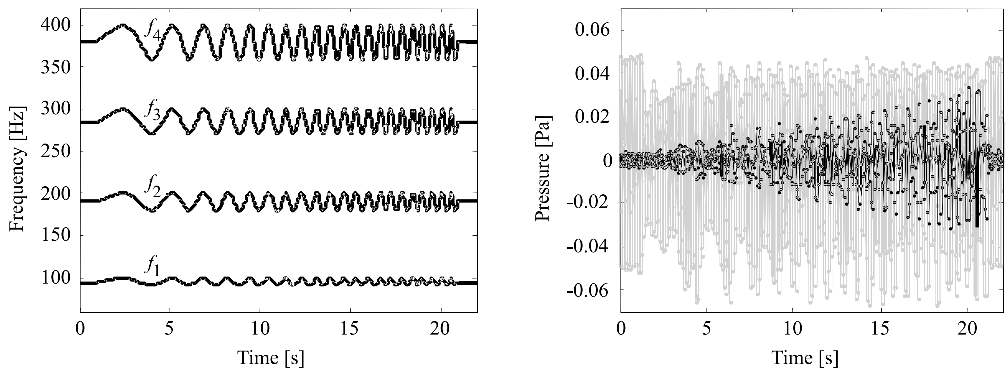

Fig. 7. Results for time-varying disturbance frequencies: Frequency variations (left) and microphone signal (right) in open loop (gray) and closed loop (black)

time interval (two times faster). At the end, the decrease from 100 Hz to 90 Hz and back to 100 Hz takes place in 1.25 seconds, which is a variation of 16 Hz per second (for rotating machinery, this would correspond to 960 rpm per second). Excellent disturbance attenuation is achieved, although it can be seen that for faster frequency variations, the disturbance attenuation decreases.

The effect of fast variations of the disturbance frequencies has been further investigated in another experiment. The results are shown in Figure 7. The disturbance frequency varies sinusoidally between the minimum and the maximum value with a variation frequency that increases from 0.1 Hz to 2 Hz over 20 seconds (left-hand side of Fig. 7). It is seen that for very fast frequency variations, the attenuation performance decreases (but the system remains stable).

7. DISCUSSION AND CONCLUSION

A discrete-time LTV controller for the rejection of harmonic disturbances with time-varying frequencies based on a state-augmented observer-based state-feedback controller with a time-varying internal model and a scheduled state-feedback gain is presented. The control design method is based on quadratic stability for pLPV systems.

The design method guarantees stability of the closed loop system also for arbitrarily fast changes of the disturbance frequencies. This is an advantage over other approaches such as adaptive filtering or heuristic gain scheduling. The experimental results show that an excellent disturbance rejection is achieved. The controller corresponds to a well-known state-space control approach which might lead to an increased acceptance of the control scheme in industrial applications. The design is carried out in discrete time and the controller can easily be implemented on real-time hardware.

Some degree of conservatism is present in this approach. Using a single quadratic Lyapunov function, i.e. introducing no limitations on the rate of change of the disturbance frequencies, limits the range of admissible disturbance frequencies that can be covered with the resulting controller. Also, the polytope that contains the uncertain parameters can be chosen much smaller and with fewer vertices than the cuboid applied here, if information on the relations between the disturbance frequencies is given, as would be the case for harmonically related frequencies. Thus, feasibility of the LMIs and the upper bound on the system performance could be improved as well as the time that is needed to compute the coordinates required for the on-line interpolation. This is important for applications where many harmonics have to be cancelled, a wide frequency range has to be covered and computational resources are limited, e.g. in automotive applications [8–10]. This will be considered in future research.

References

[1] Köroğlu H., Scherer C.W. 2008, *Robust generalized asymptotic regulation against non-stationary sinusoidal disturbances*. Proc. of the 47th IEEE Conference on Decision and Control, Cancun, December 2008, 5426–31.

[2] Kinney C.E., de Callafon R.A. 2006, *Scheduling control for periodic disturbance attenuation*. Proc. of the American Control Conference. Minneapolis, June 2006, 4788–93.

[3] Kuo S.M., Morgan D.R. 1996, *Active noise control systems*. New York, Wiley.

[4] Morari M. Zafiriou E. 1989, *Robust process control*. Englewood Cliffs, Prentice Hall.

[5] Apkarian P., Gahinet P., Becker G. 1995, *Self-scheduled H_∞ control of linear parameter-varying systems: A design example*. Automatica 31, 1251–61.

[6] Du, H., Shi X. 2002, *Gain-scheduled H_∞ control for use in vibration suppression of system with harmonic excitation*. Proc. of the American Control Conference. Anchorage, May 2002, 4668–69.

[7] Du H., Zhang L., Shi X. 2003, *LPV technique for the rejection of sinusoidal disturbance with time-varying frequency*. IEE Proc. on Control Theory and Applications 150,132–38.

[8] Bohn C., Cortabarria A., Härtel V., Kowalczyk K. 2003, *Disturbance-observer-based active control of engine-induced vibrations in automotive vehicles*. Proc. of the SPIE's 10th Annual International Symposium on Smart Structures and Materials. San Diego, March 2003. Paper No. 5049-68.

[9] Kowalczyk K., Svaricek F., Bohn C. 2004, *Disturbance-observer-based active control of transmission-induced vibrations*. Proc. of the IFAC Symposium on Advances in Automotive Control, Salerno, April 2004, 78–83.

[10] Bohn C., Cortabarria A., Härtel V., Kowalczyk K. 2004, *Active control of engine-induced vibrations in automotive vehicles using disturbance observer gain scheduling*. Control Engineering Practice 12, 1029–39.

[11] Kinney C.E., de Callafon R.A. 2007, *A comparison of fixed point designs and time-varying observers for scheduling repetitive controllers*. Proc. of the 46th IEEE Conference on Decision and Control, New Orleans, December 2007, 2844–49.

[12] Kinney C.E., de Callafon R.A. 2006, *An adaptive internal model-based controller for periodic disturbance rejection*. Proc. of the 14th IFAC Symposium on System Identification. Newcastle, Australia, March 2006, 273–78.

[13] Gruenbacher E.,Furtmueller C., del Re L. 2007, *Suppression of frequency varying periodic disturbances in continuous casting using an internal model predictor*. Proc. of the American Control Conference. New York City, July 2007, 4142–47.

[14] Köroðlu H., Scherer C.W. 2008b, *LPV control for robust attenuation of non-stationary sinusoidal disturbances with measurable frequencies*. Proc. of the 17th IFAC World Congress. Seoul, July 2008, 4928–33.

[15] Köroðlu H., Scherer C.W. 2011, *Scheduled control for robust attenuation of non-stationary sinusoidal disturbances with measurable frequencies*. Automatica 47, 504–14.

[16] Apkarian P., Gahinet P. 1995, *A convex characterization of gain-scheduled H_∞ controllers*. IEEE Transactions on Automatic Control 40, 853–64.

[17] Witte J., Balini H.M.N.K., Scherer C.W. 2010, *Experimental results with stable and unstable LPV controllers for active magnetic bearing systems*. Proc. of the IEEE International Conference on Control Applications. Yokohama, September 2010, 950–55.

[18] Dettori M., Scherer C.W. 2001, *LPV design for a CD player: an experimental evaluation of performance*. Proc. of the 40th IEEE Conference on Decision and Control. Orlando, December 2001, 4711–16.

[19] Ballesteros P., Bohn C. 2011, *A frequency-tunable LPV controller for narrowband active noise and vibration control*. Proc. of the American Control Conference. San Francisco, June/July 2011, 1340–45.

[20] Ballesteros P., Bohn C. 2011, *Disturbance rejection through LPV gain-scheduling control with application to active noise cancellation*. Proc. of the 18th IFAC World Congress. Milan, August/September 2011, 7897–902.

[21] Shu, X., Ballesteros P., Bohn C. 2011, *Active vibration control for harmonic disturbances with time-varying frequencies through LPV gain scheduling*. Proc. of the 23rd Chinese Control and Decision Conference. Mianyang, China, May 2011, 728–33.

[22] Feintuch P. L., Bershad N. J., Lo A.K. 1993, *A frequency-domain model for filtered LMS algorithms – Stability analysis, design, and elimination of the training mode*. IEEE Transactions on Signal Processing 41, 1518–31.

[23] Apkarian P. 1997. *On the discretization of LMI-synthesized linear parameter-varying controllers*. Automatica 33, 655–61.

[24] Ogata K. 1995, *Discrete-time control systems*, 2nd ed. Englewood Cliffs, Prentice Hall.

[25] Francis B., Wonham W. 1976, *The internal model principle of control theory*. Automatica 12, 457–65.

[26] Amato F. 2006, *Robust control of linear systems subject to uncertain time-varying parameters*. Berlin: Springer.

[27] Horn R. A., Johnson C.R. 1985, *Matrix analysis*. Cambridge: Cambridge UP.

[28] Gahinet P., Nemirovskii A., Laub A.J., Chilali M. 1995, *LMI control toolbox*. The Mathworks Inc.

[29] Daafouz J., Bara G.I., Kratz F., Ragot J. 2000, *State observers for discrete-time LPV systems: An interpolation based approach*. Proc. of the 39th IEEE Conference on Decision and Control. Sydney, December 2000, 4571–72.

[30] Hong J.H., Bernstein D.S. 1998, *Bode integral constraints, colocation, and spillover in active noise and vibration control*. IEEE Transactions on Control Systems Technology 6, 111–20.